

## EFFECT OF WO<sub>x</sub> OVER Ni/HYDROTALCITE CATALYSTS TO PRODUCE HYDROGEN FROM ETHANOL

J. L. Contreras<sup>1\*</sup>, M.A. Ortiz<sup>1</sup>, G.A. Fuentes<sup>2</sup>, M.Ortega<sup>3</sup>, R.Luna<sup>1</sup>, M. Gordon<sup>1</sup>, J.Salmones<sup>4</sup>, B.Zeifert<sup>4</sup>, L. Nuño<sup>1</sup> and T. Vázquez<sup>1</sup>

<sup>1</sup>Depto. de Energía, CBI, Universidad Autónoma Metropolitana-Azcapotzalco  
Av. Sn.Pablo 180 Col.Reynosa, Azcapotzalco C.P.02200 México D.F., México.

<sup>2</sup>Depto. de IPH, CBI, Universidad Autónoma Metropolitana-Iztapalapa, México, D.F., México

<sup>3</sup>Centro de Nanotecnología del IPN, UPALM, Zacatenco, México, D.F., México

<sup>4</sup>ESIQIE, Instituto Politécnico Nacional, Unidad Prof. UPALM, México, D. F., 07738, México

<sup>5</sup>Instituto Mexicano del Petróleo, Eje Central 152, México, D.F.México.

Tel: 53189065 ext 116 , Fax 53947378, mail: jlcl@correo.azc.uam.mx

\* contact email: [jlcl@correo.azc.uam.mx](mailto:jlcl@correo.azc.uam.mx)

### ABSTRACT

The effect of WO<sub>x</sub> over Ni-hydrotalcite catalysts to produce H<sub>2</sub> by ethanol steam reforming was studied. The catalysts were characterized by N<sub>2</sub> physisorption (BET area), X-ray diffraction, and Infrared and UV-vis spectroscopies. The W concentration ranged from 0.5 to 3 wt%. As W concentration increased, the intensity of XRD reflections of the Ni catalysts decreased. The porous structure of the materials consisted of parallel layers with a monomodal mesoporous distribution. The surface groups detected by IR were: -OH, Al-OH, Mg-OH, W=O and CO<sub>3</sub><sup>2-</sup>. UV-vis results suggested that Ni<sup>2+</sup> ions were substituted by W ions. The catalytic evaluations were made in a fixed bed reactor using a water/ethanol mol ratio of 4 at 450°C. Catalysts with low loadings of W (0.5 and 1%) showed the highest H<sub>2</sub> production and stability. W promoted the conversion of ethanol towards hydrogen in the case of the Ni-hydrotalcite catalysts. The reaction products were; H<sub>2</sub>, CO<sub>2</sub>, CH<sub>3</sub>CHO, CH<sub>4</sub> and C<sub>2</sub>H<sub>4</sub>. The catalysts did not produce CO.

**Key words:** Hydrogen, Ni, WO<sub>x</sub>, Hydrotalcite, Ethanol.

### 1. INTRODUCTION



Ethanol has several advantages over fossil fuel-derived hydrocarbons as a renewable source of hydrogen. It is nearly CO<sub>2</sub> neutral, it is less toxic; it can be more easily stored without significant handling risk and it can be obtained in large quantities from biomass [1-2].

The catalytic steam reforming of ethanol has been proposed to produce hydrogen. This reaction is endothermic and it only produces H<sub>2</sub> and CO<sub>2</sub> if the ethanol reacts in the most desirable way. However, undesirable products such as CO and CH<sub>4</sub> are also in general formed [1]. Other reactions may occur, such as dehydrogenation of ethanol to CH<sub>3</sub>CHO, dehydration to CH<sub>2</sub>=CH<sub>2</sub>, decomposition to CO and CH<sub>4</sub> or CO<sub>2</sub> and CH<sub>4</sub>.

CH<sub>3</sub>CHO and the CH<sub>2</sub>=CH<sub>2</sub> are intermediary products that could be formed during reaction at relatively low temperatures before the formation of H<sub>2</sub> and CO<sub>2</sub> and it is also possible to form coke over the surface of the catalyst.

The catalytic ethanol steam reforming has been reported to produce hydrogen and low amounts of CO and CO<sub>2</sub> [3-4]. Another attractive point of this reaction is related with the energy required to produce H<sub>2</sub>. An energy balance has shown that approximately 34% of the total energy obtained by hydrogen combustion is required to produce hydrogen, whereas the remaining 64% is the available energy [5].

There are several catalysts being studied in this field. In our case, we are interested in catalysts made out of hydrotalcites. This class of catalysts has high surface area, a good basic site distribution and these solids present the so-called memory effect [6-8].

The main objective of the present research was to study the effect of the addition of W (as WO<sub>x</sub>) to the hydrotalcite. The addition of WO<sub>x</sub> in catalysts with Al<sub>2</sub>O<sub>3</sub> has resulted in a high thermal stability [9]. The second objective was to study the effect of Ni metal on the surface of the catalysts. This metal is able to break C-H and C-C bonds to produce hydrogen [10-12].

## 2.- EXPERIMENTAL SECTION

### 2.1.- Catalyst Preparation

The hydrotalcite was made by coprecipitation using two salt solutions as precursors. First, in a stirred reactor a salt solution of Mg(NO<sub>3</sub>)<sub>2</sub> and Al<sub>2</sub>(NO<sub>3</sub>)<sub>3</sub> (J.T. Baker) with a molar ratio of 2:1



was made. A second solution of  $\text{Na}_2\text{CO}_3$  (5%) and  $\text{NaOH}$  ( $\text{pH} = 10$ ) (Carlo Erba) was prepared. These two solutions were added simultaneously drop by drop to a third stirred reactor using water as solvent (60 drops/min) at  $60^\circ\text{C}$  maintaining an atomic ratio of  $\text{Mg}^{2+}/\text{Al}^{3+}$  of 1.55. After aging the precipitate for 24 h the resulting solid was impregnated with  $\text{Ni}(\text{NO}_3)_2$ .

The solution of  $\text{Ni}(\text{NO}_3)_2$  was added in such a way as to get a constant amount of 1 wt% Ni. The precipitate was washed, dried and calcined at  $450^\circ\text{C}$  for 5h. These solids were impregnated with a solution of  $(\text{NH}_4)_{12}\text{W}_{12}\text{O}_{41} \cdot 5\text{H}_2\text{O}$ , (Aldrich) having different W concentrations: 0 wt% W and 1%Ni (sample HTN), 0.5wt% W and 1%Ni (HTN05W), 1wt% W and 1wt%Ni (HTN1W), 2wt% W and 1wt%Ni (HTN2W), 3 wt% W with 1wt%Ni (HTN3W). The impregnation of the solids was made during 24 h at  $60^\circ\text{C}$ . The solids were washed, dried at  $120^\circ\text{C}$  for 24 h and calcined at  $450^\circ\text{C}$  during 5 h. Finally the samples were reduced with pure  $\text{H}_2$  at  $500^\circ\text{C}$  for 2 h.

## 2.2.- Catalysts Characterization

The solids obtained were characterized by X-ray diffraction (XRD) in a Phillips X' Pert instrument. The XRD patterns of the samples after calcination were obtained using the  $\text{CuK}\alpha$  radiation. Diffraction intensity was measured in the  $2\theta$  range between  $5$  and  $70^\circ$  with a  $2\theta$  step of  $0.02^\circ$  with 8 seconds per point, the samples were analyzed directly at room temperature. The infrared spectroscopy was made in a Perkin Elmer spectrophotometer (Spectrum-RX). An infrared beam was sent through a wafer of the sample. The wavenumber range was from  $4000$  to  $400\text{ cm}^{-1}$  and the number of scans averaged was 50.  $\text{N}_2$  physisorption at 77 K was made in a Micromeritics 2000 instrument. Each sample was pretreated at  $200^\circ\text{C}$  under vacuum ( $1 \times 10^{-4}$  torr). The diffuse reflectance UV-visible spectroscopic analysis (UV-vis) of the samples was made in a Varian (Cary 5E) spectrophotometer. The range of wavelength was from  $3000$  to  $200\text{ nm}$ .

## 2.3.- Catalytic evaluation for steam reforming of ethanol.

The catalytic reaction was made in a U-shaped stainless steel fixed bed reactor. The catalyst (1g, 100 US mesh) was charged for each of the reaction evaluation. The feed of the reactants



consisted of ethanol (Aldrich), water as steam and  $N_2$  (purity 99.99%, Infra-Air Products).  $N_2$  was fed through a micrometric needle valve (1 ml/s). The gas mixture of  $H_2O$  and  $CH_3CH_2OH$  (molar ratio of 4/1) in  $N_2$  stream was prepared using two glass saturators followed by heating to  $92^\circ C$  before it was feed to the reaction chamber.

The temperature of the catalyst was raised at  $500^\circ C$  in flow of  $N_2$  for 30 min to clean the catalyst surface and then the flow of reactants started at  $450^\circ C$ . The catalyst was held at that temperature for 30 min in order to make three analyses. In the case of deactivation tests the catalysts were evaluated during 420 min.

The analysis of the reactants and all the reaction products was carried out online by gas chromatography. Inside an automated injection valve, the sample was divided into two portions which were then analyzed in order to obtain accurate, complete quantification of the reaction products. One sample was used to analyze  $H_2$ ,  $CO$ ,  $CO_2$  and  $CH_4$ , using a packet column of silica gel 12 grade 60/80 (18'x 1/8") with a thermal conductivity detector (Gow-Mac apparatus). The second sample was used to analyze  $CH_3CH_2OH$ ,  $CH_3CHO$ ,  $CH_3COCH_3$ ,  $CH_2O$  and  $CH_2=CH_2$  with a capillary column (VF-1ms, 15m x 0.25 mm) in a Varian chromatograph CP-3380 with a flame ionization detector (FID). Response factors for all products were obtained and the system was calibrated with appropriate standards before each catalytic test. The conversion (X) was calculated using the ethanol composition before and after of the reaction. The selectivity of each product was defined as follows:  $S_i (\%) = N_i / \sum N_j \times 100$  (see the nomenclature).

### 3.- RESULTS AND DISCUSSION

#### 3.1.- Textural properties

The surface area (BET) and the nominal content of W are shown in Table 1. These samples were mesoporous [6] and they showed the a IV type hysteresis (Figure 1) according to the IUPAC classification [13-15]. The hysteresis of the isotherms corresponded with the structure of parallel plates typical of the hydrotalcites [16]. The surface area obtained in the Ni series was nearly inversely proportional to the W concentration. This  $WO_x$  effect was similar with that observed in



WO<sub>x</sub> /Al<sub>2</sub>O<sub>3</sub> catalysts [9], although we did not detect surface oxo compounds by Raman spectroscopy in our samples at low W concentrations. It could be possible that WO<sub>x</sub> species were inside the hydrotalcite structure. This possibility was strengthened by the fact that the pore volume decreased as the W concentration increased.

**Table 1.** Surface area BET and W concentration of the WO<sub>x</sub>/ Ni-Hydrotalcite catalysts

Catalysts	W (% wt)	Surface area BET (m <sup>2</sup> /g)	Pore volume (cm <sup>3</sup> /g)	Pore diameter (Å)
HTN	0	226	0.23	578
HTN05W	0.5	197	0.14	254
HTN1W	1	223	0.16	254
HTN2W	2	195	0.14	469
HTN3W	3	159	0.12	450

The sample without W (sample HTN) showed the widest pore distribution (50 to 1000 Å) having an average pore diameter of 578 Å (Figure 2), while the samples with the lowest W content: 0.5 and 1 wt% W (HTN05W and HTN1W) had a small average pore diameter of 254 Å. In these two samples the highest effect of W occurred on the pore diameter. These results suggest that the WO<sub>x</sub> interacted with the hydrotalcite structure in the interlayer space producing pores smaller than the pores obtained without W. Further addition of tungsten to the hydrotalcite (samples HTP2W and HTP3W) produced samples with pore diameter between that obtained of the HTN sample and those of the samples HTN05W and HTN1W. We observed the largest interaction of WO<sub>x</sub> with the hydrotalcite structures at low W concentrations (0.5 and 1 wt% W).





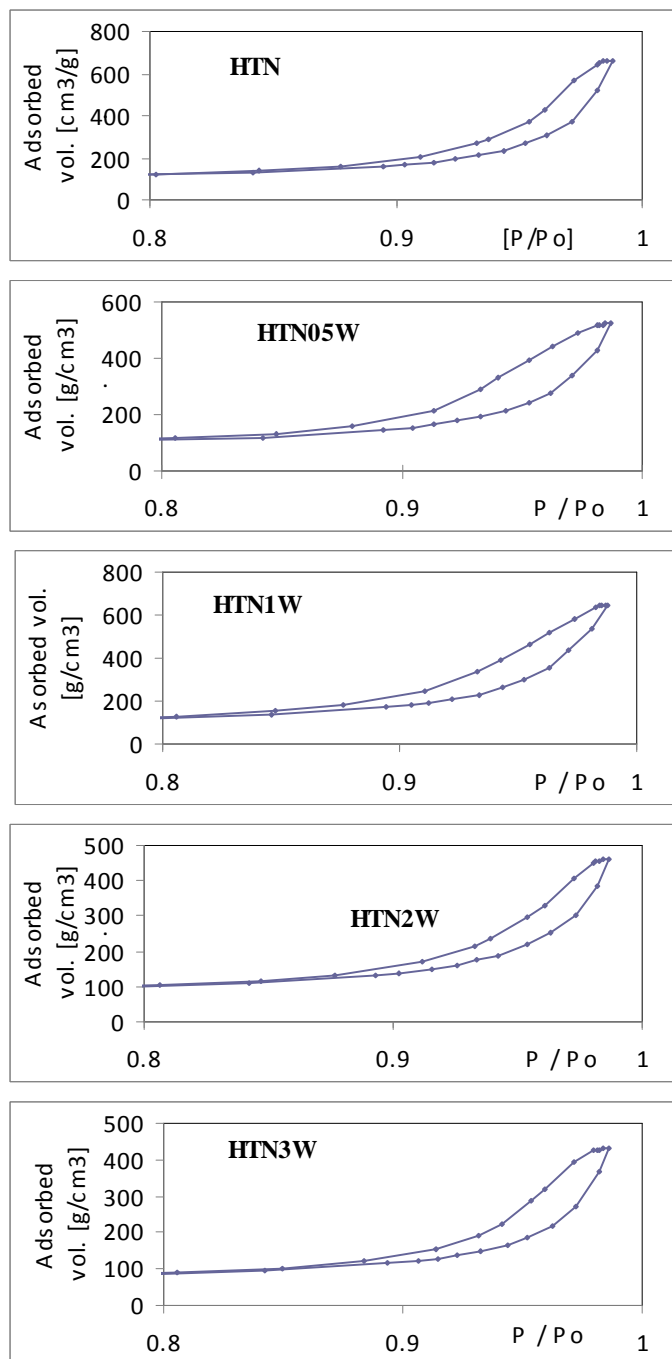
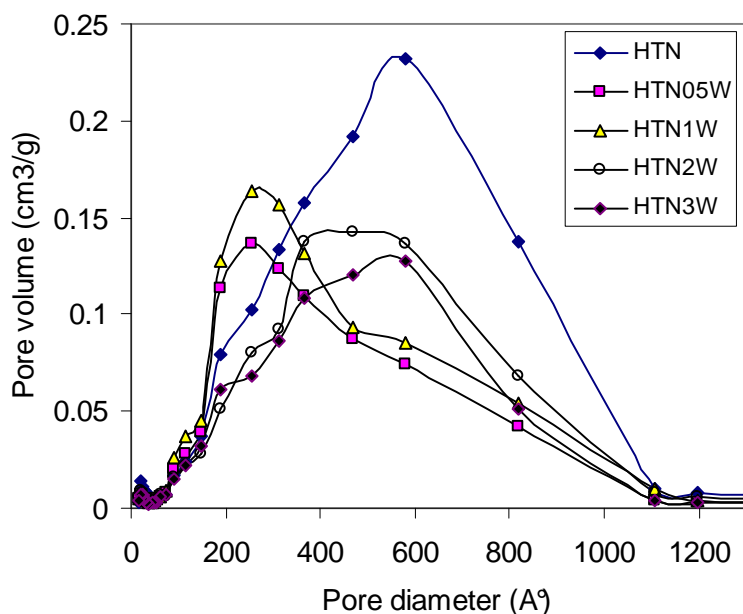


Figure 1.  $\text{N}_2$  isotherms ( hysteresis) for  $\text{WO}_x/\text{Ni}$ -hydrotalcite catalysts.



**Figure 2.** Pore distribution of the WO<sub>x</sub>/Ni-hydrotalcite catalysts.

### 3.2.- XRD analysis

For samples with Ni XRD showed symmetric intense peaks corresponding to (003), (006), (110) and (113) reflections (Figure 3). Additionally, we observed asymmetric peaks with smaller intensity in (012), (015) and (018). These peaks correspond to a laminar structure typical of hydrotalcites [16]. At larger W concentration the crystalline structure of the samples decreased. The absence of other phases suggests that both W<sup>6+</sup> and Al<sup>3+</sup> have isomorphically replaced the Mg<sup>2+</sup> cations in the burcite (Mg(OH)<sub>2</sub>) - like layers [6, 10,13,17]. The intensity of the diffraction lines assigned to the hydrotalcite phase decreased by the addition of W ions, suggesting a decrease in the population of Mg-Al-Hydrotalcite structures. The Ni<sup>+2</sup> and Mg<sup>+2</sup> exchange could be possible [18], but that is difficult to ascertain with the low Ni concentration used.



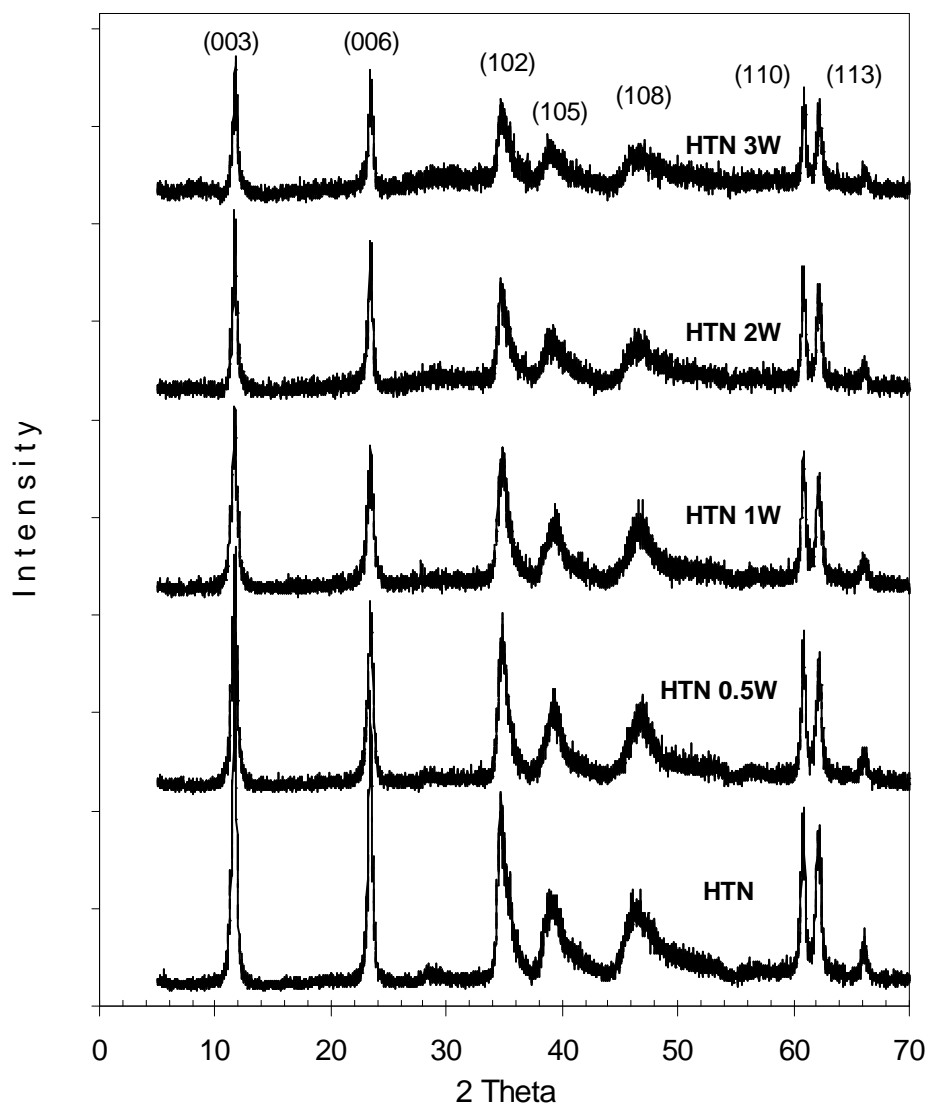


**Figure 3.** XRD of the WO<sub>x</sub>/Ni-hydrotalcite catalysts.

### 3.3.- Infrared spectroscopy

The infrared spectra for the samples with Ni are shown in Figure 4. They present a broad OH stretching band in the 3100-3700 cm<sup>-1</sup> region and the H<sub>2</sub>O scissoring mode band near 1600 cm<sup>-1</sup> provides evidence for the presence of water molecules. Other authors have attributed the band at 3410 cm<sup>-1</sup> to hydroxyl groups coordinated with Mg and Al, while the vibration of the same group





associated with water is a wide band between  $3650\text{--}3590\text{ cm}^{-1}$  [19]. The absorbance values (calculated by  $A = 2.3 - \log_{10} \% T$ ) for this band were: 0.83, 0.73 and 0.77 for catalysts HTN2W, HTN3W and HTN 0.5W whereas 0.57 and 0.47 for catalysts HTN and HTN1W. The lowest absorbance was for the catalyst having 1 wt% W. This suggests that this catalyst had the lowest amount of hydroxyl groups  $\text{--OH}$ .

A strong band located at  $1380\text{ cm}^{-1}$  is attributed to the presence of residual nitrate ions. Another band located at  $1029\text{ cm}^{-1}$  is related with the symmetric  $\text{C=O}$  stretching carbonate ion which has been found in  $1041\text{ cm}^{-1}$  [20]. In the region below  $1000\text{ cm}^{-1}$  the spectrum showed a band located in  $772\text{ cm}^{-1}$  assigned to  $\text{--OH}$  bending vibrations of brucite ( $\text{Mg(OH)}_2$ ) type layers [20].

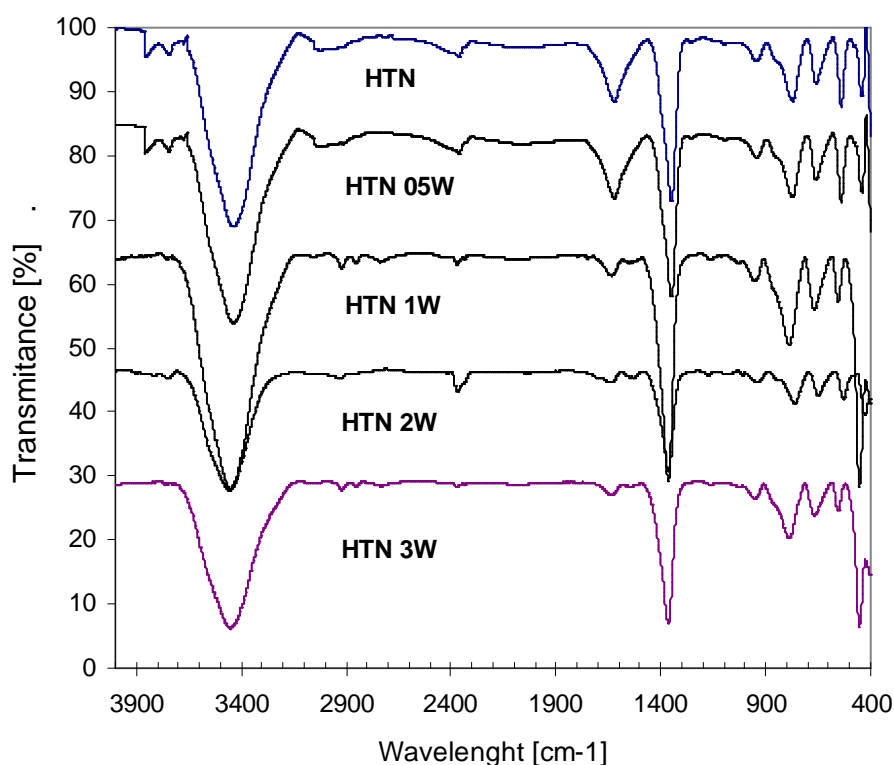


**Figure 4.** Infrared spectra of the  $\text{WO}_x/\text{Ni}$ -hydrotalcite catalysts

The bands located at  $680$  and  $560\text{ cm}^{-1}$  correspond to vibration modes of brucite-type layers, specifically the metal-oxygen symmetrical stretching. The antisymmetric  $\text{--OH}$  stretching band



located at  $3460\text{ cm}^{-1}$  decreased as the W concentration increased, and so did the  $\text{H}_2\text{O}$  scissoring mode band at  $1600\text{ cm}^{-1}$ . These results suggest that some of the  $-\text{OH}$  groups in the brucite type layers of the hydrotalcite could be substituted by  $\text{WO}_x$  species.

### 3.4.- UV-vis spectroscopy

The strong band between 200-300 nm increased as W concentration increased (Figure 5) and it has been attributed to a ligand-metal charge transfer (LMCT) of the single ligand in  $\text{W}=\text{O}$  [21, 22]. In the case of  $\text{Al}_2\text{O}_3$  this band increased with the W concentration, and the  $\text{W}^{6+}$  was present in a tetrahedral coordination [23-25].

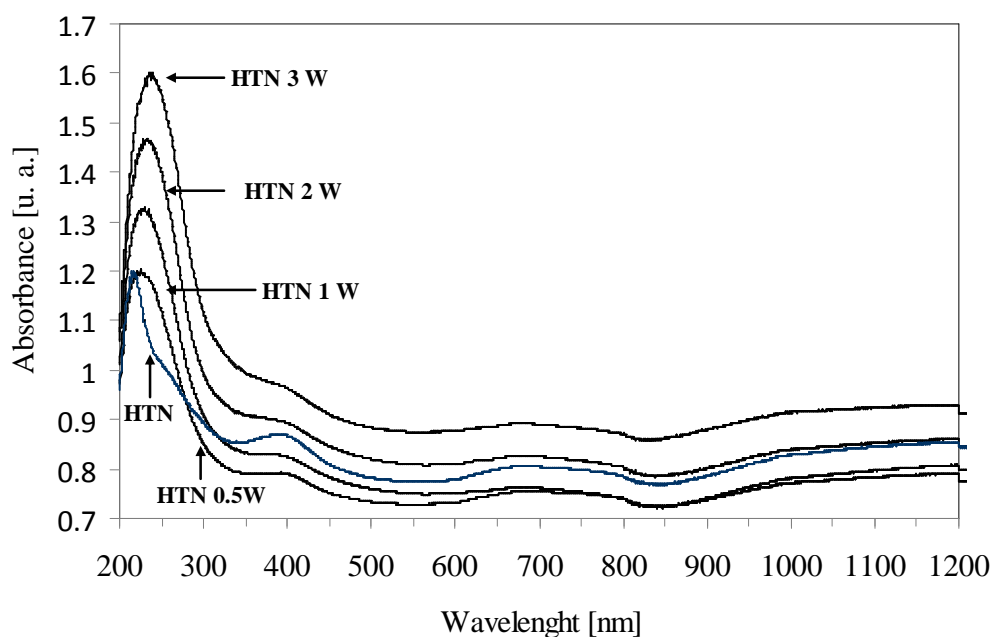


**Figure 5.** UV-vis spectra of the  $\text{WO}_x/\text{Ni}$ -hydrotalcite catalysts

It is known that the structure of the tungstate ion  $[\text{W}_{12}\text{O}_{41}]^{12-}$  in aqueous solution is highly dependent on the pH [26]. In alkaline solutions  $\text{W}^{6+}$  is present as a tetrahedral monomeric ion  $[\text{WO}_4]^{2-}$ . This may apply in our case, as the hydrotalcites have a basic nature.



The band between 350-450 nm is a d-d transition band assigned to the Ni-O group of NiO [27]. The band located between 650-721 nm could be ascribed to  $\text{Ni}^{2+}$  ions in octahedral coordination [27] in a  $\text{NiAl}_2\text{O}_4$  -type spinel-like structure formed through diffusion of Ni ions into the support. These bands decreased as the  $\text{W}^{6+}$  ions increased, probably by substitution of Ni ions by W ions.

### 3.5.- Catalytic activity

We observed a small promotion effect by addition of 0.5 wt % W to the Ni-hydrotalcite (Figure 6). The products of reaction were  $\text{H}_2$ ,  $\text{CH}_3\text{CHO}$ ,  $\text{CO}_2$ ,  $\text{CH}_4$  and  $\text{CH}_2=\text{CH}_2$  (shown in Figure 7).

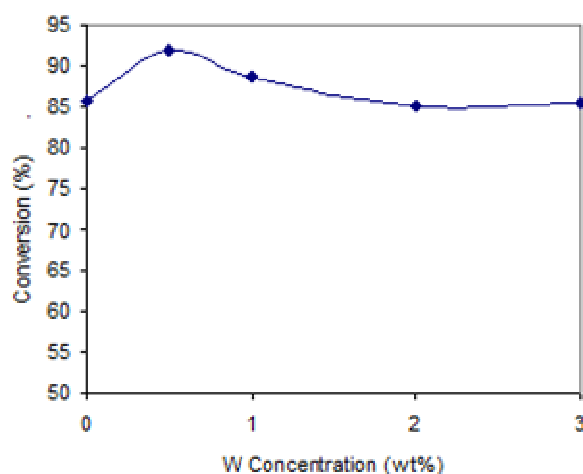


**Figure 6.** Effect of W concentration over the conversion for the  $\text{WO}_x/\text{Ni}$ -hydrotalcite catalysts at 450°C

Ni-hydrotalcite (HTN) catalyzes ethanol steam reforming (Figures 6 and 7) as reported elsewhere [20] and the amount of Ni was not critical in the range studied. For this type of catalysts, the production of ethylene, acetaldehyde and diethyl ether vanishes at 500°C and above.

The presence of surface  $-\text{OH}$  on the catalyst has been reported to be important to catalyze the initial interaction of ethanol with these  $-\text{OH}$  groups to form ethoxy species [28] which could evolve to  $\text{CH}_3\text{CHO}$ . This compound may evolve over the surface through alkyl elimination or by forming a bidentate acetate species, which through C-C scission can produce  $\text{CO}_2$ ,  $\text{CH}_4$  and  $\text{H}_2$  in the presence of water. This explanation may be similar for the steam reforming of ethanol using ZnO. This oxide has showed catalytic activity producing  $\text{H}_2$ ,  $\text{CO}_2$  and  $\text{CH}_3\text{CHO}$  [28].



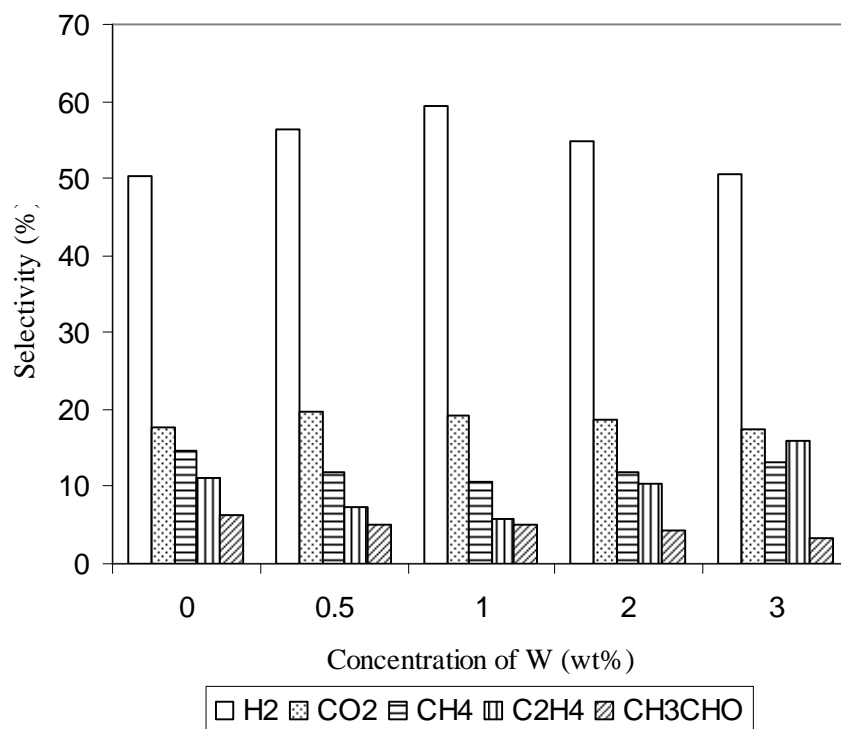
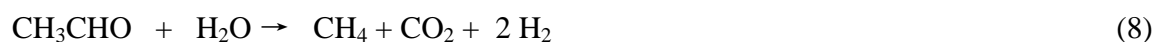
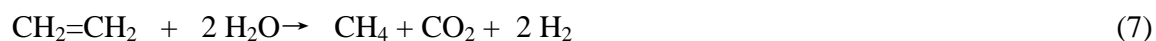
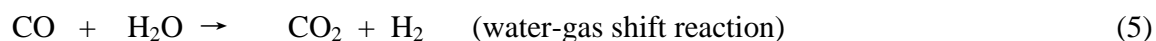
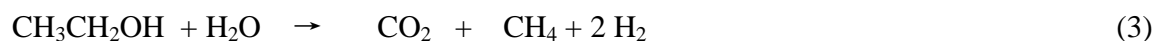


**Figure 7.** Reaction products from-WO<sub>x</sub>/Ni-Hidrotalcite catalysts at 450°C

The reaction products in Figure 7 are produced in accordance with the following reactions:



We found  $\text{CH}_3\text{CHO}$  with all the catalysts studied, suggesting that  $\text{WO}_x/\text{Ni}$ -hydrotalcite surface acted as a dehydrogenation catalyst according to reaction (2).

Hydrogen was the main product with several reactions contributing to its production (mainly reaction 1). We did not detect CO perhaps because it reacted with water to produce  $\text{CO}_2$  and more  $\text{H}_2$  in accordance with reaction (5) or because reaction (1) was more favored than reactions (3) and (6) which are the route for CO production. Although some CO can be produced at thermodynamic equilibrium it may not be relevant in continuous operation because the methane reforming reaction (6) is not favored at temperatures below  $450^\circ\text{C}$  and it is also kinetically limited. Therefore, the most relevant reactions describing results from Figure 7 are reaction (1), (2) and (3) and (4).

The ethanol dehydration to  $\text{CH}_2=\text{CH}_2$ , reaction (4) was affected by the presence of W. The catalyst with the highest W concentration showed the highest production of ethylene. In this point, the distribution of dehydration products (ethylene and diethyl ether) was dependent on both Ni and W concentrations. It has been reported [20] that for Ni-hydrotalcite catalysts, the higher the Ni loading, the lower is the selectivity to ethylene and diethyl ether. It may be possible that in our catalysts surface Ni sites could be substituted by W ions as suggested by our UV-vis spectroscopy results. If this occurred, a decrease in the concentration of Ni sites on the catalyst would favor the selectivity to the dehydration products. Additionally, it is important to remember that the presence of these products could lead to the formation of coke [29], and their yield has a space-time dependence typical of intermediate products [30].

The difference in  $\text{H}_2$  mole fraction between all the catalysts was small and  $\text{H}_2$  production comes from several reactions; dehydrogenation, water-gas shift conversion of CO and decomposition of oxygenated compounds. Infrared studies have shown that dehydrogenation of molecularly adsorbed ethanol was a key reaction step [31].

Ethanol adsorbs molecularly to form weakly adsorbed hydrogen-bonded species and to produce strongly adsorbed molecular ethanol on the Lewis-sites of the support. It was found that high temperature treatment of the adsorbed species caused the formation of surface acetate species on



the support. The presence of water lowered the temperature for the appearance of acetate species and increased the stability of monodentate ethoxide species.

The HTN1W catalyst showed the highest production to  $H_2$  and the lowest production to  $C_2H_4$  (Figure 7) and moreover, it did not deactivate during 7 h on-stream (see section 3.7).

### 3.6.- Equilibrium calculations

To get an idea of the approach to equilibrium, we performed calculations considering that reaction (1) represents the main contribution in the system [32]. Figure 8 shows the equilibrium mole fractions for the different components calculated from equation 9 using equations 10-18 to define mole fractions. We considered the 4:1 molar flow ratio of water to ethanol.

$$K = \frac{y_{CO_2}^2 y_{H_2}^6}{y_{H_2O}^3 y_{OH}} \quad (9)$$

The mole balance of the reaction (1) was as follows:

$$N_{OH} = (N_{OH}^\circ - N_{OH}^\circ X) \quad (10)$$

$$N_{CO_2} = N_{OH}^\circ 2X \quad (11)$$

$$N_{H_2} = N_{OH}^\circ 6X \quad (12)$$

$$N_{H_2O} = (N_{H_2O}^\circ - N_{OH}^\circ 3X) \quad (13)$$

$$N = \text{Total mole flow} = N_{OH}^\circ + 4N_{OH}^\circ X + N_{H_2O}^\circ \quad (14)$$

The mole fractions were:

$$y_{OH} = (N_{OH}^\circ - N_{OH}^\circ X) / N \quad (15)$$

$$y_{CO_2} = (N_{OH}^\circ 2X) / N \quad (16)$$

$$y_{H_2} = (N_{OH}^\circ 6X) / N \quad (17)$$

$$y_{H_2O} = (N_{H_2O}^\circ - N_{OH}^\circ 3X) / N \quad (18)$$



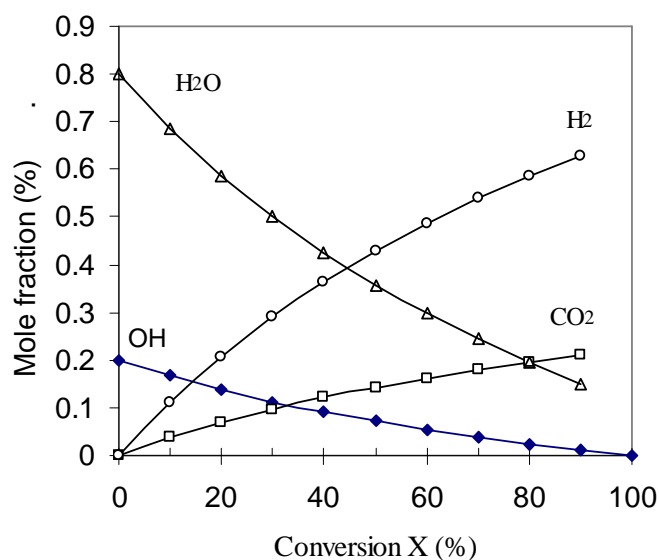


**Figure 8.** Mole fractions  $y_i$  for each reaction product in the equilibrium calculated from de Equation (9).

The experimental and equilibrium mole fractions for  $H_2$ ,  $CO_2$ , and  $H_2O$  were compared (Table 2). Only small differences were found independently of the catalyst used, suggesting that the reaction is equilibrium controlled.

Table 2. Experimental<sup>1</sup> and equilibrium mole fractions of some reaction products (considering only reaction (1)) for the  $WO_x/Ni$ -hydrotalcite catalysts at 78% conversion.

Catalyst	$C_2H_5OH$		$H_2$		$CO_2$		$H_2O$	
	Exper.	Calculated	Exper.	Calculated	Exper.	Calculated	Exper.	Calculated
HT05W	0.026	0.008	0.50	0.592	0.17	0.20	0.14	0.20
HTN05W	0.033	0.008	0.56	0.592	0.19	0.20	0.15	0.20
HTN1W	0.042	0.008	0.59	0.592	0.19	0.20	0.17	0.20
HTN2W	0.051	0.008	0.54	0.592	0.18	0.20	0.17	0.20
HTN3W	0.068	0.008	0.50	0.592	0.17	0.20	0.21	0.20

<sup>1</sup> The experimental mole fractions of the  $CH_3CHO$ ,  $C_2H_4$  and  $CH_4$  were not included



### 3.7.- Catalytic Stability

The catalysts HTN05W and HTN (0.5 and 0 wt% W) showed good stability during 7 h on-stream tests at 450°C (Figure 9). This behavior was similar to the W effect in catalysts of Pt supported on  $\text{Al}_2\text{O}_3$  [10, 32]. In those studies, low concentrations of tungsten oxides (below monolayer, W < 1 wt %) stabilized thermally the  $\text{Al}_2\text{O}_3$ , as they do the hydrotalcite in this study.

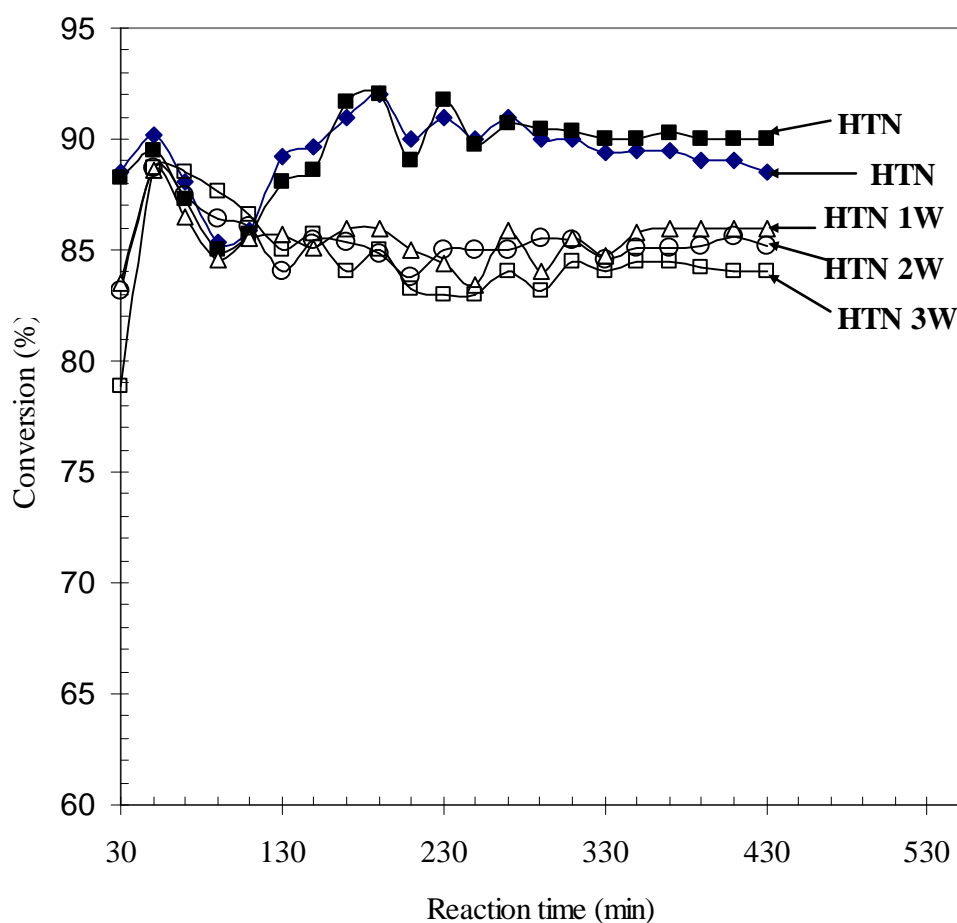


**Figure 9.** Long term reactions on  $\text{WO}_x/\text{Ni}$ -Hydrotalcite catalysts at 450°C



#### 4.- CONCLUSIONS

The porous structure of the  $\text{WO}_x$ -Ni-hydrotalcite catalysts involves parallel layers with a monomodal mesoporous distribution. It appears that Ni ions were substituted by W ions according to UV-vis spectroscopy. The surface groups determined by IR include  $\text{H}_2\text{O}$ , Al-OH, Mg-OH and  $\text{CO}_3^{2-}$ .

We observed a small promotion effect of W at low W concentrations on the Ni/hydrotalcite catalysts. The addition of 0.5 wt % W increased the selectivity to  $\text{H}_2$  and the conversion, with the selectivity being the highest for the catalyst with 1 wt%. The catalysts studied did not produce CO and showed low selectivity to ethylene. Experimental and calculated equilibrium mole fractions of  $\text{H}_2$  were close for the catalysts studied. The catalyst with the lowest W concentration was slightly more stable than the catalyst without W. Catalysts with W concentrations higher than 0.5 wt% W did not show a promotion effect during long time-on-stream tests.

#### 5.- NOMENCLATURE

$S_i$  (%) = Selectivity to product i

$N_i$  = Moles of product i

$N_j$  = Moles of each product (included i)

K = Equilibrium constant

$y_{\text{CO}_2}$  = Mole fraction of  $\text{CO}_2$

$y_{\text{H}_2}$  = Mole fraction of  $\text{H}_2$

$y_{\text{H}_2\text{O}}$  = Mole fraction of  $\text{H}_2\text{O}$

$y_{\text{OH}}$  = Mole fraction of Ethanol

#### 6.- ACKNOWLEDGEMENTS

The authors acknowledge the financial support of the Universidad Autónoma Metropolitana-Azcapotzalco and -Iztapalapa, the Instituto Politécnico Nacional and the Instituto Mexicano del Petróleo.



## 7.- REFERENCES

- [1] R.D. Cortright, R.R. Davda, J.A. Dumesic, *Nature* **418**, 964(2002).
- [2] J. Llorca, N.Homs, J.Sales, J.L. G. Fierro and P.Ramírez de la Piscina, *J. Catal.* **222**,470-480(2004).
- [3] A. Aboudheir, A. Akande,R. Idem, A. Dalai, *Int. J. of Hydrogen Energy* **31**,752-761(2006).
- [4] Kurt Koelling, Fuel Cell Grade Hydrogen Production from the Steam Reforming of Bio-Ethanol Over Co-based catalysts: *An Investigation of Reaction Networks and Active Sites. Ph.D. Thesis, The Ohio State University, (2005).*
- [5] M.A. Ortiz R., *Obtención de hidrógeno a partir de bioetanol empleando catalizadores de Co, Ni y Pt sobre hidrotalcitas, estabilizados con WOx, Tesis UAM-Azcapotzalco, (2009).*
- [6] M. de los Ángeles Ocaña Z. *Síntesis de Hidrotalcitas y Materiales Derivados: Aplicaciones en Catálisis Básica. Tesis de Doctorado, Universidad Complutense de Madrid. (2005).*
- [7] H. Liandro Reza G., *Síntesis y caracterización fisicoquímica de catalizadores sólidos básicos tipo hidrotalcita de cobalto y níquel. Tesis de licenciatura, Universidad Autónoma Metropolitana, Unidad Azcapotzalco (2003).*
- [8] F. Cavan, F. Trifiro,A.Vacari, *Catal. Today*,**11**, 173-301(1991).
- [9] J.L.Contreras, G.A.Fuentes, J.Salmones, B. Zeifert, *J. of Alloys and Compounds* **483**, 371-373(2008).
- [10] J.L.Contreras, J.Salmones, L.A. García, A. Ponce, B. Zeifert and G.A. Fuentes, *J. of New Materials for Electrochemical Systems* **11**, 109-117(2008).
- [11] M.N. Barroso, M.F. Gómez, L.A. Arrúa, M.C. Abello, *Appl. Catal. A:General* **304**, 116-123(2006)
- [12] J. Llorca, N.Homs, J.Sales, and P.Ramírez de la Piscina, *J. Catal.* **209**, 306-317(2002)
- [13] K. Sing, D. Everett, R. Haul, L. Moscou, R. Pierotti, J. Rouquerol, and T. Siemieniewska, *Pure Appl. Chem.* **57**, 603 (1985).
- [14] L. D. Gelb, K. E. Gubbins, R. Radhakrishnan, and M. Sliwinska-Bartkowiak, *Reports on Progress in Physics* **62**, 1573 (1999).



- [15] S. Lowell, J. E. Shields, M. A. Thomas, and M. Thommes, *Characterization of Porous Solid and Powders: Surface Area, Pore Size and Density*, Kluwer Academic Publishers, 2004.
- [16] M. del Arco, D. Carriazo, S. Gutiérrez, C. Martín and V. Rives, *Inorg. Chem.* **43**, 375-384(2004).
- [17] A.C.C. Rodríguez, C.A. Enríquez, J.L.F. Monteiro, *Mater. Res.* **6**, 563(2003).
- [18] T. Shishido, M. Sukenobu, H. Morioka, R. Furukawa, H.I Shirahase, K. Takehira, *Catal. Lett.* **73**, 21(2001).
- [19] María de los Ángeles Ocaña Zarceño, *Síntesis de Hidrotalcitas y Materiales Derivados: Aplicaciones en Catálisis Básica. Tesis de Doctorado, Universidad Complutense de Madrid* (2005).
- [20] C. Resini, T. Montenari, L. Barattini, G. Ramis, G. Busca, S. Presto, P. Riani, R. Marazza, M. Sisani, F. Marmottini, U. Costantino, *Appl. Catal. A: General*, **355**, 83-93(2009).
- [21] A. Bartecki and Dembicka, D. *J. of Inorg. and Nuclear Chem.* **V.29, I.12**, 2907-2916(1967).
- [22] J.L. Contreras and G.A. Fuentes, *Studies in Surface Science and Catalysis, Vol. 101 Edit. B. Delmon and J.T. Yates, Elsevier* **1195-1204** (1996).
- [23] A. Iannibello, L. Villa, and S. Marengo, *Gazzetta Chimica Italiana*, **109**, 521(1979).
- [24] L. Salvati, L.E. Makovsky, J.M. Stencel, F. R. Brown, D.M. Hercules, *J. Phys. Chem.* **85**, 3700-3707(1981).
- [25] J.A. Horsley, I.E. Wach, J.N.M. Brown, G.H. Via, F.D. Hardcastle, *J. Phys. Chem.* **91**, 15 4014-4020 (1987).
- [26] W.P. Griffith and T.D. Wickins, *J. Chem. Soc. A.* **1087**(1966).
- [27] S. Damyanova, B. Pawelec, K. Arishtirova, J.L.G. Fierro, *International Journal of Hydrogen Energy*, **36**, 10635-10647 (2011)
- [28] J. Llorca, N. Homs, P. Ramírez de la Piscina, *J. of Catal.* **227**, 556-560(2004).
- [29] J.R. Rostrup-Nielsen, N. Hojlund in: J. Oudar, H. Wise (Eds.), *Deactivation and Poisoning of Catalyst*, Marcel Dekker, New York, Basel, **p.57** (1985).



- [30] J.Comas, F. Mariño, M.Laborde, N. Amadeo. *Chem Eng. J.* **98**, 61-68(2004).
- [31] A. Erdohelyi, J. Rasko, T. Kecskes, M. Toth, M.Dömök, K.Baán, *Catal. Today* **116**,367-376(2006).
- [32] J. L. Contreras, M.A. Ortiz, G.A. Fuentes, R. Luna, J. Salmones, B. Zeifert, L. Nuño and A.Vázquez, *J. of New Materials for Electrochemical Systems*, **13**, 253-259 (2010).